Indian J Phys. **81 (9)** 851-869 (2007)

IJP

Computational strategies for redox processes in condensed phase : Both explicit and implicit solvation treatments

Nital Mehta and Sambhu N Datta*

Department of Chemistry Indian Institute of Technology Bombay Powai Mumbai 400 076 India

E mail sndatta@chem iitb ac in

Abstract : We provide a detailed account of the theory of solvation models, especially those involved in the calculation of the reduction potentials of biomolecules in a solvent or a membrane The explicit solvation model involves a hybrid quantum mechanical-molecular mechanical (QM/MM) treatment of the solvated biomolecule and a dynamical treatment of the primary solvent layer through either Molecular dynamics (MD) or Monte-Carlo (MC) simulations Contributions of the solvent molecules in the bulk to the free energy change of the reduction process is incorporated in the form of the Born free energy of ion-dielectric interaction, the Onsager energy of dipole-dielectric interaction and the Debye-Huckel energy of ion-ionic cloud interaction The implicit solvation treatment employs the dielectric polarisable continuum model (DPCM) where all the solvent molecules together are represented as a continuum with a fixed dielectric constant Whereas the implicit model only accounts for an average molecule medium interaction, the explicit model also considers fluctuations of the medium molecules from their average coordinates in thermal equilibrium

The theory and the models are exemplified by calculations on three biomolecules in different environments The QM/MM method could successfully reproduce the standard reduction potential of plastocyanin in water The QM/MM/MD + Born/Onsager/Debye-Huckel procedure was used to obtain the standard oxidation and reduction potentials of Chlorophyll-*a* in acetonitrile The QM/MM/MC + Born/Onsager/Debye-Huckel technology was adopted to determine the one- and two-electron reduction potentials of Pheophytin-*a* in DMF The implicit solvation model along with density functional treatment (DFT-DPCM method) was also used to this end A finite difference Poisson-Boltzmann solver along with the DFT-DPCM method was utilized to calculate the reduction potential of Pheophytin-*a* within the thylakoid membrane These examples amply demonstrate the soundness of the explicit and implicit models of molecule-medium interaction

Keywords : Biomolecules, reduction potential, QM/MM/MC/MD, DFT-DPCM

PACS Nos. : 02 70 Bf, Ns, Ss, 31 15 A-, E-, 71 15 Pd, 74 25 jb

1. Introduction

Over the recent years, extensive work has been carried out on the theoretical investigation of the electron transport route for the light phase of photosynthesis [1–4]. Newton *et al* investigated electron transfer reactions in condensed phases [5]. A density matrix model of photosynthetic electron transfer with microscopically-based

*Corresponding Author

estimates of vibrational relaxation times was prepared by Parson and Warshel [6]. Our group has successfully obtained the standard oxidation and reduction potentials of chlorophyll-*a* in acetonitrile and the reduction potential of plastocyanin in water by employing the hybrid quantum mechanical-molecular mechanical (QM/MM) methodology [7]. Our activity in this field involves (1) a thermodynamic study of the biomolecules occurring in the Z-scheme of photosynthesis, specifically, the computation of redox potential values of these molecules *in vivo* and *in vitro*, and (2) the calculation of the rate of electron transfer between two biomolecules within the condensed phase of the thylakoid membrane [8(a)].

This paper gives a detailed account of the theory and methodology we adopted to calculate the reduction potential of a general molecule in a specific medium. The redox potential of a reaction is related to the free energy change by a simple equation. The free energy change of a reaction involves a large number of energy terms like electronic, thermal and solvation energies which are required to be evaluated. The evaluation of the solvation energy incorporating the molecule-medium interaction is of prime importance here. We give an account of the theory involved, and illustrate how different solvation models can be obtained from the general treatment.

We discuss both the explicit and implicit solvation models to calculate the solvation energy term. As the name suggests, the explicit solvation treatment is based on considering the dynamics of each associated solvent molecule explicitly. The implicit solvation treatment is based on treating the solvent implicitly as a dielectric continuum, thereby evaluating the effect of solvent molecules. Furthermore, we discuss the finite difference Poisson-Boltzmann (FDPB) solver along with the Density Functional Theory–Dielectric Polarizable Continuum Model (DFT-DPCM method) to obtain the reduction potential values within a membrane.

As an example, we show how the above methods have been successfully employed to obtain the one-electron reduction potential of plastocyanin in water, [7(g)] oxidation and reduction potentials of chlorophyll-*a* in acetonitrile [7(h)] and one- and two-electron reduction potentials of Pheophytin-*a* in the solvent N,N-dimethyl formamide (DMF). We have also calculated the one-electron reduction potential of Pheophytin-*a* within the thylakoid membrane [9].

2. Theory

The interaction of molecules and a medium is an area that has attracted attention for a long time, since the early days of chemistry. Many researchers, both chemists and physicists, have contributed to the gaining of a theoretical understanding of the modification of properties of molecules in a medium, a solvent, and a rigid or semi-rigid condensed phase. One of the earliest theoretical advances was made by Max Born [10] who calculated the free energy of an ion interacting with a dielectric continuum from classical electrostatics. Another classical advancement was made by Lars Onsager [11] in the calculation of the free energy of interaction between a dipole

and a dielectric continuum. Onsager's treatment was quantum mechanical, and the so-called Onsager free energy is in reality a first-order correction. Born's treatment was purely classical, but in the same spirit it can be viewed as a first-order one.

A very comprehensive and succinct quantum statistical theory of molecule-medium interaction was constructed by Jack Simons [12]. The basic problem is to solve the Schrödinger equation for the whole molecule-medium system which is to be statistically averaged over the thermal equilibrium of all molecules of the medium that are moving all the time. There are standard techniques of quantum statistical mechanics to take care of such averaging [13]. Simons and Banerjee [14] mostly investigated the spectral changes on solvation. In one instance, McHale and Simons [15] studied the transport of a solvated electron.

In a recent publication [16], it has been demonstrated that the Simons theory, after being updated for the kinetic motion of the solute, gives rise to the general transport equations for a fluid medium. In particular, the quantum Langevin equation and the Fokker-Planck equation can be derived from the quantum statistical mechanical treatment suggested by Simons.

Besides, use has been made of the updated Simons theory to study the propagation of excitation energy in a molecular crystal [8]. This has been applied to the numerical investigation of excitation transport in thylakoid membrane [17]. The calculated results thereof have been used to solve, for the first time, the kinetics of the very complicated process of production of glucose equivalents in C4 plants [18].

2.1. Hamiltonian :

The Hamiltonian for the solute molecule can be written as [16]

$$h_{\text{sol}}(\{\boldsymbol{r}\}) = h_{\text{internal}}(\{\boldsymbol{r}\}) + \boldsymbol{p}_{\text{cm}}^2/2M\,. \tag{1}$$

In the above, $\{\boldsymbol{r}\}$ represents the internal coordinates, $\boldsymbol{p}_{\text{cm}}$ is the linear momentum operator for the center of mass, and M is the total mass of the solute.

The medium Hamiltonian is represented as a sum of kinetic energy and interaction energy for all the molecules of the medium,

$$h_{\text{med}}(\{\boldsymbol{R}\}) = T(\{\boldsymbol{P}\}) + U(\{\boldsymbol{R}\}). \tag{2}$$

Here $(\{\boldsymbol{R}\}, \{\boldsymbol{P}\})$ stands for the phase space coordinates of the medium molecules. The solute-medium interaction is written as

$$u\big(\{\boldsymbol{r}\},\ \boldsymbol{r}_{\text{cm}},\ \{\boldsymbol{R}\}\big) = u_0 + \delta V\big(\{\boldsymbol{r}\},\ \boldsymbol{r}_{\text{cm}},\ \{\boldsymbol{R}\}\big)\,. \tag{3}$$

It contains information on the internal modes of the solute. The term u_0 represents the ground state stabilization energy of the solute in medium. The interaction δV accounts for the variation of the potential energy as each solvent molecule moves from one location to another. It arises from the fluctuation of the medium coordinates from their equilibrium values.

The total molecule-medium Hamiltonian is

$$H = h_{sol} + h_{med} + u . \tag{4}$$

It can be partitioned as

$$H = H^0 + \delta V \tag{5}$$

where

$$H^0 = h_{internal} + h_{cm} + h_{med} + u_0 \tag{6}$$

The perturbation δV is small in thermal equilibrium at a relatively low temperature.

At this point we make clear how our treatment of transport [8,16,17] fundamentally differs from the treatment of Simons [14]. The difference is in the kinetic energy term of the solute (or the exciton in a thermal bath) which we included in our formalisms in the past, and without which the transport cannot be envisaged.

The grand canonical distribution operator for the medium is defined by

$$\hat{\rho}_{med} = e^{-\beta(h_{med} - \mu_{med} N_{med})} / \mathrm{Tr}\left\{ e^{-\beta(h_{med} - \mu_{med} N_{med})} \right\}, \tag{7}$$

where μ_{med} is the chemical potential of the solvent molecules and N_{med} is the corresponding number. One observes

$$u_0 = \mathrm{Tr}\left\{ \hat{\rho}_{med} u(\{r\}, r_{cm}, \{R\}) \right\} . \tag{8}$$

The distribution operator of the solute is not explicitly considered here as the solute electronic excitation occurs at very high energy values. The solute molecule is nevertheless considered to be in thermal equilibrium thus accounting for its average translational, rotational and vibrational energies.

2.2. The u_0 effect :

The classical Born energy and the semiclassical Onsager energy can be viewed as arising from the average interaction u_0. Let the unperturbed wave functions for the solute and the medium be ψ^0_{sol} and ψ^0_{med}. The isolated solute-isolated medium complex has the wave function $\Psi^0_{complex} = \psi^0_{sol}\, \psi_{med}$, with ψ_{med} representing the thermal ground state of the medium. It is possible to write the average value over ψ_{med} by using the average values of the medium eigenstates ψ^0_{med}'s and the distribution operator ρ_{med}. The interaction u perturbs the wave functions of the solute, medium and the complex. The perturbed functions are ψ_{sol}, ψ'_{med} and $\Psi_{complex}$, the last one being not necessarily a simple product of ψ_{sol} and ψ'_{med}.

2.2.1. Born and Onsager energies :

Both Born energy and Onsager energy can be obtained as first order corrections. First of all, u perturbs the solvent wave function. The perturbed solvent interacts with the solute charge distribution.

The Born energy [10] is obtained by considering that the statistically averaged interaction u_0 is given from classical electrostatics,

$$u_0^B = \frac{q^2}{2a_0\varepsilon} \tag{9}$$

where q is the charge of the solute, a_0 is its radius, and $\varepsilon(T)$ is the temperature-dependent dielectric constant. The statistical averaging is embedded into the dielectric constant. Since u_0^B is a constant term, one obtains the Born energy correction

$$E_B^{(1)} = \left\langle \Psi_{\text{comple}}^{(0)} \; u_0^B | \Psi_{\text{complex}}^{(0)} \right\rangle = u_0^B \tag{10}$$

Notice that the correction is always positive. By comparing with the energy correction in vacuum for which the dielectric constant is 1, one obtains the Born free energy of solvation as

$$G_{\text{Born}} = u_0^B(\varepsilon) - u_0^B(1) = -\frac{q^2}{2a_0}\left(1 - \frac{1}{\varepsilon}\right. \tag{11}$$

When the solute molecule or ion is electrically unsymmetrical, it is associated with a net (ground state) electrical dipole moment ($\vec{\mu}_0$). The net charge, if non-zero, leads to a net Born free energy of solvation. But the net charge polarization does not give any contribution to Born free energy. It still interacts with the solvent, by polarizing it. In turn, the polarized solvent dipoles create a reaction field ($\vec{\varepsilon}_R$) at the center of the solute dipole,

$$\vec{\varepsilon}_R = \frac{2(\varepsilon - 1)}{2\varepsilon + 1}\frac{\vec{\mu}_0}{a_0^3}. \tag{12}$$

The solute dipole interacts with the reaction field as

$$u_{0,\text{sol}}^O = \frac{1}{2}\vec{\mu}.\vec{\varepsilon}_R = \frac{(\varepsilon - 1)}{2\varepsilon + 1}\frac{\vec{\mu}.\vec{\mu}_0}{a_0^3} \tag{13}$$

where $\vec{\mu}$ is the solute dipole moment operator, and a_0 now is the radius of the spherical cavity in which the solute dipole resides. The dielectric medium exists outside this cavity.

In Onsager's treatment, energy correction to the medium is also evaluated. After statistical averaging, one obtains

$$u_{0,\text{med}}^O = -2u_{0,\text{sol}}^O. \tag{14}$$

Therefore, the total average interaction is given by

$$u_0^O = u_{0,\text{sol}}^O + u_{0,\text{med}}^O = -u_{0,\text{sol}}^O. \tag{15}$$

The first order energy correction is then written as

$$G_{\text{Onsager}} = E_{\text{O}}^{(1)} = \left\langle \Psi_{\text{complex}}^{(0)} \middle| u_0^{O} \middle| \Psi_{\text{complex}}^{(0)} \right\rangle = -\frac{(\varepsilon - 1)}{2\varepsilon + 1} \frac{\mu_0^2}{a_0^3} \cdot \tag{16}$$

2.2.2. Polarized continuum model :

This method is a quantum mechanical treatment of solute-dielectric interaction, first proposed by Newton [5(a)]. In principle, one evaluates the interaction of the solute charge density distribution with the dielectric continuum by solving the Schrödinger equation in a self-consistent manner. One deals with ψ_{sol}, ψ'_{med} and Ψ_{complex}. From the interaction energy computed, one subtracts $u_0^{\text{B}}(1)$ if there is a net non-vanishing change of the solute.

The PCM method has several characteristic features. (1) A molecule is rarely spherical, or even approximately spherical, in shape. The PCM method considers an effective shape and an effective volume. It adds half a diameter of solvent to the isolated molecule boundary. In practice, in most cases the solvent is water, and 0.5 Å is added. This gives rise to the forbidden boundary, outside of which the dielectric continuum is considered. The use of 0.5 Å for water may lead to a slight error, especially for other solvents. In any case, no spherical approximation is made for the molecular shape. (2) The PCM method relies on self-consistency. Therefore, the results are in principle valid for all orders. However, the basic quantum mechanical calculation may be carried out at various levels like mean-field, density functional treatment, second, third or fourth order perturbation theory, *etc.* (3) In general, one finds results closely tallying with $E_B^{(1)}$ and $E_0^{(1)}$, when the parameters a_0 for eqs. (9) and (13) are very well estimated. One also observes the theoretical soundness, $E_{O,\text{med}} = -2E_{O,\text{sol}}$. (4) The PCM method also allows molecular geometry optimization. Thus the geometry in a medium differs from that of an isolated molecule. (5) The PCM method also estimates non-electrostatic contributions like cavitation, dispersion and repulsion energies.

Because of these characteristics, the PCM calculations are able to generate representative numbers for solvation energy.

The PCM method visualizes the medium as a uniform dielectric. All statistical averaging are contained in $\varepsilon(T)$. So, this method does not explicitly account for any fluctuation from the average solvent polarization.

2.3. The δV effect :

The fluctuation δV at any instant of time is the difference between the actual interaction u at that instant and the average interaction u_0. The quantity δV may be viewed as the dielectric fluctuation. However, it goes beyond this point of view. The solvent molecules generally have other multipoles. Therefore, it is best to want a description of the solvent molecules explicitly and not by an average description of a dielectric medium. One would like to make an explicit calculation on the solute-solvent complex, with random orientations of the molecules of the medium, and then finally

make a statistical mechanical averaging of the energies for different conformations of the solvent molecules. In practice, one considers a finite number of associated solvent molecules and considers the same to constitute the primary solvation shell. The effect of the innumerable solvent molecules in the bulk is then estimated as the very small Born free energy and the Onsager energy of the solute-primary solvation layer complex.

Presently, the number considered for the associated solvent molecules varies from 25 to 200. It is envisaged that with the advent of computing power and speed one will be able to consider a few thousands of the associated solvent molecules in the near future.

2.3.1. ONIOM – the u_0 effect :

An explicit treatment of solvent molecules around a solute involves a large number of atoms, so a quantum mechanical computation of their energy requires a huge amount of time and is thus impractical. To reduce the computing time without greatly affecting the accuracy, Morokuma *et al.* [19] employed the ONIOM (our **O**wn **N**-layer **I**ntegrated molecular **O**rbital molecular **M**echanics) method.

ONIOM is a hybrid method which divides the system into several onion-like layers, treating the active center with the highest level *ab initio* QM method while outer layers can be treated with less expensive methods, such as low-level *ab initio* QM, semi-empirical QM, or MM methods. The two-layer ONIOM (high : low) is an approximation to the energy of the real system at the high level. The energy is given by

$$E_{\text{real}}^{\text{ONIOM}} = E_{\text{model}}^{\text{high}} + E_{\text{real}}^{\text{low}} - E_{\text{model}}^{\text{low}} \tag{17}$$

where 'high' and 'low' refer to the high- and low-level theoretical methods. The quotes 'model' and 'real' refer to the active site and the whole system respectively.

Two different approaches exist for the treatment of electrostatic interaction between the QM and MM layers. These two approaches are (1) ONIOM with mechanical embedding (ONIOM-ME) and (2) ONIOM with electrostatic embedding (ONIOM-EE).

ONIOM-ME : In this method, the electrostatic interaction is included in the MM calculation. The energy expression is

$$E_{\text{real}}^{\text{ONIOM-ME}} = E_{\text{model}}^{\text{high}} + E_{\text{real}}^{\text{MM}} - E_{\text{model}}^{\text{MM}}. \tag{18}$$

Here $E_{\text{real}}^{\text{MM}}$ includes the molecular mechanics electrostatic interaction in the full (real) system (ES_{real}). ES_{real} is given by

$$ES_{\text{real}} = \sum_{J<K}^{\text{real}} \frac{s_{JK} q_J q_K}{r_{JK}} \tag{19}$$

where q_J is the partial charge on the atom J, r_{JK} is the distance between atoms J and K, and summation J and K are for all the atoms in the system. Also, s_{JK} is the

scale factor of electrostatic interaction introduced in most force field definitions (independent of the ONIOM or QM/MM applications).

ONIOM-EE : In the electrostatic embedding, one includes the electrostatic interaction between the QM charges and the MM part as additional scaled electrostatic Hamiltonian H' of the QM systems,

$$H'_{\text{model}} = -\sum_{i}\sum_{J}^{\text{MM}} \frac{\sigma_J q_J}{r_{iJ}}, \tag{20}$$

where i refers to the electrons in the system and the individual MM atomic charges are scaled by a factor σ_J. One additional term, representing the energy of interaction between the nuclei of the active site and the MM atomic charges, is also considered Here polarization of the wave function of the QM region by the MM atomic charges occurs. ONIOM-EE is better in describing a very polar system compared to ONIOM-MM. The EE scheme is more expensive as it requires a self-consistent charge iteration.

By the ONIOM method, we can obtain the optimized geometry of a molecule in the presence of the associated solvent molecules for a particular conformation, giving the energy of a static system. The solvent conformation can also vary, and the optimized geometry for the most stable solute-solvent complex conformation can be determined. This accounts for the term u_0.

2.3.2. Dynamical solvent – the δV effect :

In order to incorporate the dynamic nature of the solvent molecules during the energy calculation, Molecular dynamics (MD) or Monte-Carlo (MC) simulations are carried out within a theoretical volume or box. A constant temperature is maintained. Periodic boundary conditions are then applied. Mulliken charges are assigned to all the atoms present within the box. If the solute has a net charge, suitable counterions are to be placed among the solvent molecules. The solvent molecules are initially optimized under a molecular mechanics force field, and then allowed to relax for some-time in MD and for a regular *max delta* (maximum trial atomic displacement) in MC. The geometry of the biomolecular solute is kept fixed during the simulations. The system is allowed to reach equilibrium for sometime. Thereafter, the energy values are noted. A Boltzmann average of all the energy values is then carried out to obtain the energy of the dynamic primary solvent layer. This treatment gives an account of the average kinetic energy of the solvent molecules and the fluctuation (δV effect).

3. Methology

The main task is to obtain the difference of electronic, thermal and solvation energy of the charged form of a molecule from its neutral form in the presence of a solvent or any other polarisable medium. From the difference in the above energy terms, the free energy change (ΔG^0_{red}) of a particular reaction can be obtained. The mid-point

redox potential for a particular reaction can then be obtained from the knowledge of the free energy change involved in that process and the free energy change involved at the hydrogen electrode. The latter quantity has been determined by Reiss and Heller and also by Cramer *et al* [20(a-b)].

3.1. Geometry optimization :

It is necessary to consider the effect of the surrounding solvent molecules on the geometry of the molecule during optimization. As discussed in the earlier section, this can be achieved in two ways. First, one may consider the solvent molecules explicitly *via* QM/MM approach. The second way is to treat the solvent molecules implicitly *via* the polarisable continuum model (DFT-DPCM). Gaussian 03 (G03) suite of programs [21] can be used in all the calculations on optimizing the geometry of the solvated species.

3.2. Thermal energy and molecular entropy :

The thermal energy and molecular entropy are obtained by carrying out frequency calculations on the truncated model of the porphyrin ring for both chlorophyll-*a* [7(h)] and pheophytin-*a* [9]. The truncated model has been adopted for the following reasons : (1) most of the quantum chemical softwares calculate the vibrational frequencies by normal mode analysis of small molecules involving not more than 50 atoms; (2) frequency calculations on large molecules are computationally expensive; and (3) as the contribution of the difference in thermal energy towards the free energy change of a reduction process is very small (a few electron volts) compared to the contribution of the electronic energy term, the adoption of a truncated model that retains the major features of the electronic structure differences between the neutral species and its ions is very well justified. The molecular geometry of each model system with different charges must be separately optimized at first, and the optimized geometries are to be used for normal mode frequency analysis.

3.3. Explicit solvent treatment (QM/MM/MD or QM/MM/MC method) :

We have employed the QM/MM method with mechanical embedding [19].

3.3.1. Electronic energy :

In the QM/MM/MD or QM/MM/MC method, the neutral and charged forms of the solute molecules are optimised by the ONIOM method [19,22] at ROB3LYP (restricted open shell Becke 3-parameter Lee, Yang and Parr exchange correlation functional) level using a medium size basis set like 6-31G(d) and the solvent molecules are treated by the universal force field (UFF) [23]. Electronic energies of the biomolecules are finally obtained by carrying out single point calculations employing a larger basis set like 6-311 + G(2d,2p) on the ONIOM optimized geometries.

3.3.2. Solvation energy :

We employ both the explicit (QM/MM/MD + Born/Onsager/Debye-Hückel and

QM/MM/MC + Born/Onsager/Debye-Hückel) model and implicit solvation model (DFT-DPCM) to account for the contribution of the solvent molecules to the free energy change of the reduction process.

In the QM/MM/MD model, several different solvent configurations are considered around chlorophyll-*a*. To incorporate the dynamic nature of the primary solvent layer, MD simulations are carried out. A constant temperature ensemble is adopted and the initially optimized solvent layer is allowed to relax for 30 ps. Then an MD simulation of 60 ps is performed. A time step of 0.001 ps is adopted for the simulations and around 6000 data points are averaged by Boltzmann distribution to obtain the interaction energy of the biomolecule with the primary solvent layer. Periodic boundary condition is applied and Mulliken ROB3LYP/6-31G(d) charges are adopted on all the atoms.

In the QM/MM/MC model, the primary solvent shell of about 45 solvent molecules is treated in a constant volume (cubic unit cell of volume of about 25 × 25 × 25 $Å^3$) at a constant temperature (298.15 K). The solvent molecules around the neutral and charged species are initially optimized under the molecular mechanics (CHARMM 27) force field by employing the Steepest Descent algorithm. The optimized configuration is then allowed to relax at a regular *max delta* (maximum trial atomic displacement) of 0.05 Å. A total of 1000 run steps is carried out. The system is allowed to reach equilibrium for the first 300 run steps. Data are collected after each run step thereafter. A Boltzmann average was carried out on the remaining 700 data points. Mulliken charges obtained at the ROB3LYP/6-31G(d) level are used for the solvent molecules and also for the neutral and charged forms of Pheophytin. Periodic boundary condition is applied to mimic the entire system and to remove the finite boundary effects. One and two Na^+ ions were introduced at the centre of the box to neutralize the charges of the anion and dianion respectively. Hyperchem Professional Release 7 for Windows [24] can be used in these calculations.

3.3.3. Perturbative corrections to solvation energy :

The remaining solvent bulk is treated as a structureless dielectric continuum. The contribution of these layers towards the free energy change of the reduction process is incorporated by suitable Born, Onsager and Debye-Hückel corrections.

The Born free energy of the ion-dielectric interaction is given by eq. (11), where a_0 is the radius and q is the total charge of the solute-primary-solvation-layer complex. The quantity ε is the dielectric constant of the bulk solvent.

The Onsager free energy of the dipole-dielectric interaction is given by eq. (12), where μ is the ground state dipole moment of the solute-layer complex.

The additional stabilization provided by the medium through the ion-ionic atmosphere interaction is estimated by using Debye-Hückel theory. We write

$$G_{DH} = -\frac{Q^2\kappa}{2\varepsilon}. \qquad (21)$$

The Debye-Hückel reciprocal length κ is given by

$$\kappa = \left[\frac{4\pi e_0^2}{\varepsilon k_B T}\sum_i\left(\frac{Nc_i}{1000}\right)z_i^2\right]^{1/2} \tag{22}$$

where e_0 is the electronic charge, k_B is the Boltzmann constant, T is the temperature of the system in Kelvin, N is the Avogadro number, c_i is the concentration of the i-th species in molar unit, and $z_i e_0$ is the charge of the i-th ion [25]. We take 1M concentration for each type of the ions (with the corresponding ionic strength 1 M for anionic solution and 4 M for dianionic solution).

For a specific process in a solvent medium,

$$\Delta G^0_{red} = \Delta(E)_{model,QM} + \Delta E_{thermal} + (\Delta G_{MC} + \Delta G_{Born} + \Delta G_{Onsager} + \Delta G_{DH}) - T\Delta S \tag{23}$$

neglecting the PV contribution as it is negligibly small for solvated species. Gaussian 03 is employed to obtain the values of a_0 and μ of the neutral and charged forms of the biomolecule–solvent complex at ROB3LYP/6-31G(d) level.

3.4. Implicit solvent treatment (DFT-DPCM method) :

3.4.1. PCM (polarisable continuum model) [26] :

In the DFT-DPCM (Dielectric Polarizable Continuum Model) method, single point SCRF calculations are carried out employing the ROB3LYP methodology at 6-311+G(2d,2p) level. These calculations are performed on the vacuum optimized geometries of both the neutral and charged forms at ROB3LYP/6-31G(d) level.

3.4.2. Alternative calculation of medium interaction energy :

We have also calculated the free energy change of a reduction process within the thylakoid membrane. The finite difference Poisson–Boltzmann (FDPB) method [27,28] along with the DFT-DPCM method were used to obtain the electrostatic and non-electrostatic contributions toward the free energy change of the reductive process within the membrane.

We then obtain

$$\Delta G^0_{red} = \Delta G_{el} + \Delta G_{non\text{-}el}. \tag{24}$$

3.5. Standard reduction potential :

The standard reduction potential is written as

$$E^0_{red}(\text{in V}) = -\frac{1}{n_e}\left[\Delta G^0_{red}(\text{in eV}) - \Delta G^0_{H^+/(1/2)H_2(g)}(\text{in eV})\right] \tag{25}$$

where n_e is the number of electrons transferred in the half-cell reaction and the ΔG^0 values are quantities per molecule.

4. Application

The above methodologies have successfully reproduced the reduction potential of Plastocyanin (PC) in water [7(g)] Chlorophyll-*a* (Chl) in acetonitrile [7(h)] and Pheophytin-*a* (Pheo-*a*) in DMF and within the thylakoid membrane [9].

In the active site of Plastocyanin, the Cu atom is co-ordinated by the N^{δ} (imidazole) atoms of His 37 and His 87, the S^{γ} (thiolate) atom of Cys 84, and the S^{δ} (thioether) atom of Met 92 as shown in Figure 1(a). There are 140 and 141 atoms in Chl-*a* and Pheo-*a* as shown in Figures 1(b) and 1(c) respectively.

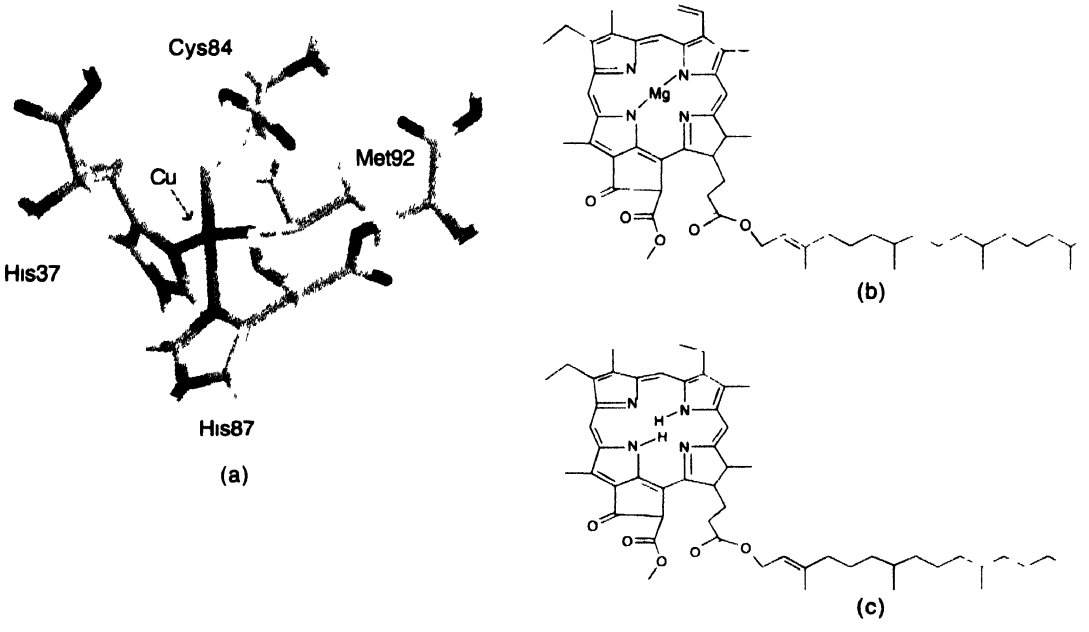

Figure 1. Structure of the active sites of (a) Plastocyanin, (b) Chlorophyll-*a* and (c) Pheophytin-*a* (Reproduced with permission from *J. Phy. Chem.* **B108** 8007 (2004); **B109** 9066 (2005) and **B111** 7210 (2007). Copyright (2004), (2005) and (2007) American Chemical Society).

For computational purposes, we worked on the truncated forms PC-76, Chl-46, Chl-85, Pheo-47 and Pheo-86, species with 76, 46, 85, 47 and 86 atoms respectively. Chl-46 and Pheo-47 have the vinyl group intact and all the other side chains replaced by hydrogen atoms. Chl-85 and Pheo-86 retain all the side chains intact except that the phytyl chain is replaced by an ethyl group.

The thermal energy and molecular entropy values for the neutral and charged forms of Plastocyanin, Chl-*a* and Pheo-*a* are obtained by carrying out frequency calculations at ROB3LYP/6-31G(d) level on their vacuum optimized geometries. The reasons for the adoption of the truncated model for the frequency calculation has

already been explained in Section 2. The optimized geometries employed for thermal energy calculations are shown in Figures 2(a), 2(b) and 2(c) respectively.

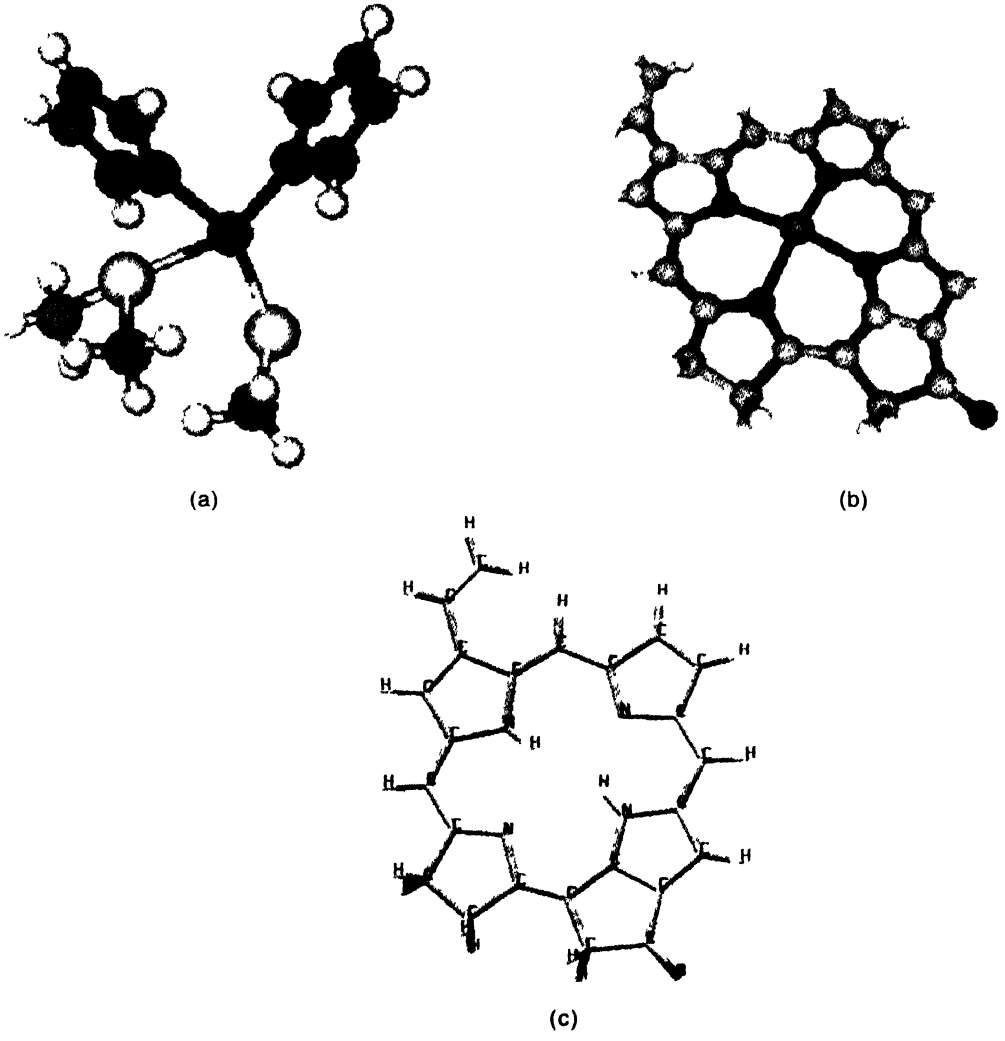

Figure 2. Gas phase optimized geometry of the models used for frequency calculations of (a) Plastocyanin, (b) Chlorophyll-*a* and (c) Pheophytin-*a*. Chl-46 and Pheo-47 have all substituents except the vinyl group replaced by hydrogen atoms. (Reproduced with permission from *J. Phy. Chem.* **B108** 8007 (2004); **B109** 9066 (2005) and **B111** 7210 (2007). Copyright (2004), (2005) and (2007) American Chemical Society).

For the ONIOM calculations on Plastocyanin in water, Chl-*a* in acetonitrile and Pheo-*a* in DMF, we optimized the structure of PC-76, Chl-85 and Pheo-86 in the presence of the respective solvents. Snapshots of the three biomolecules along with the primary solvation shell of respective solvent molecules are given in Figures 3(a), 3(b) and 3(c) respectively. The geometry was optimized employing the ONIOM methodology at ROB3LYP/6-31G(d) : UFF level. The primary solvation shell was further treated by MD or MC simulation.

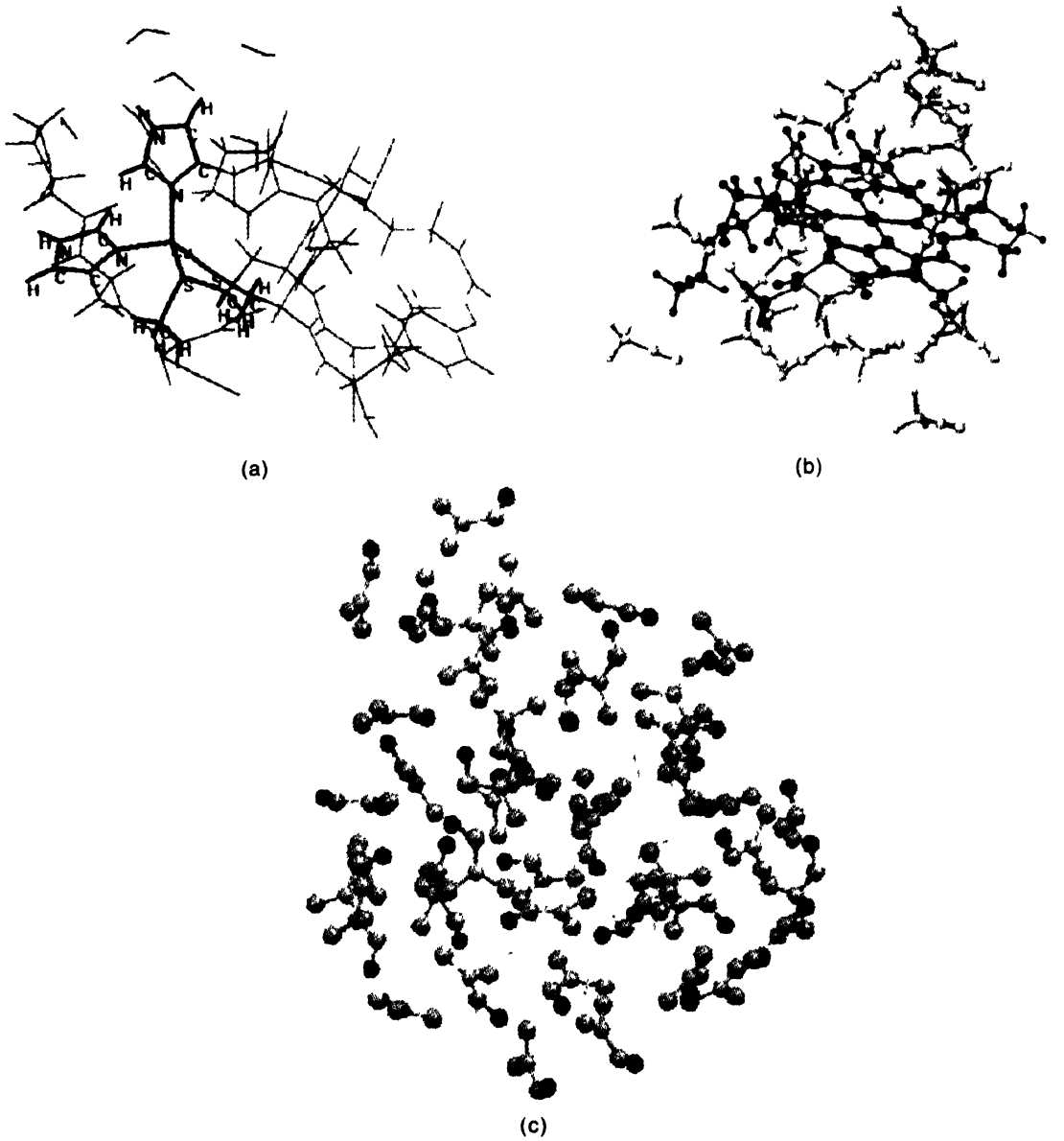

Figure 3. Biomolecules with primary solvation shell of solvent molecules. For the sake of clarity, hydrogen atoms are not shown here. (Reproduced with permission from *J. Phy. Chem.* **B108** 8007 (2004); **B109** 9066 (2005) and **B111** 7210 (2007). Copyright (2004), (2005) and (2007) American Chemical Society).

In the DFT-DPCM method we employed the vacuum optimized geometries of the neutral and charged species at ROB3LYP/6-31G(d) level.

To obtain the reduction potential value of Pheophytin-*a* within the thylakoid membrane, we have chosen a section of the overall structure of PSII from 2AXT entry in the Brookhaven Protein Data Bank. This section includes all the proteins and cofactors within a radial distance of 4 Å from Pheo-*a*. The following residues are

present : (a) 4 units of LEU, 4ALA, 1THR, 2ILE, 3PHE, 2TYR, 1GLN, 2PRO, 1MET, 1GLY, 1VAL, 1TRP; (b) 2 molecules of CLA (Chlorophyl-*a*), 1MGE [(1S)-2-(alpha-L-allopyranosyloxy)-1-[tridecanoyloxy)methyl] ethyl palmitate]; and (c) 1PHO (Pheophytin-*a*). All the co-ordinates were taken from the crystal structure of Pheophytin-*a* (PDB code : 2AXT) (Figure 4).

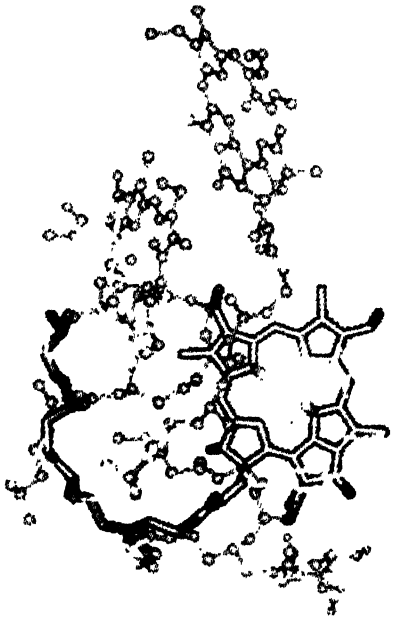

Figure 4. A section of the overall structure of PSII (from 2AXT entry in the Brookhaven Protein Data Bank). The truncated model consists of (a) 4 units of LEU, 4ALA, 1THR, 2ILE, 3PHE, 2TYR, 1GLN, 2PRO, 1MET, 1GLY, 1VAL, 1TRP (shown as narrow sticks); (b) 2 molecules of CLA, 1MGE (shown in ball and stick model); and (c) 1PHO (shown as broad lines). (Reproduced with permission from *J. Phy. Chem.* **B111** 7210 (2007). Copyright 2007 American Chemical Society).

In the truncated model, the cleaved peptide linkages were converted to free carboxylic (COO^-) or free amino (NH_3^+) groups, as required. The WHAT IF software [29] is used to insert both polar and non-polar hydrogen atoms into the amino acid and only the polar hydrogen atoms into the cofactors. The co-ordinates of the inserted hydrogen atoms was then optimized by the MM+ force field. The FDPB method was applied on the above truncated model. Radius was assigned to all the protein atoms from the Delphi [30] database (CHARMM22 parameter set). Partial charges on all the atoms in the proteins was assigned by employing the CHARMM22 parameter set while the DFT electrostatic-potential (DFT-ESP) charges derived by the CHelpG scheme at the ROB3LYP/6-31G(d) level were used for all the cofactors. The grid spacing was set to 0.29 Å, that is, there were 3.5 grid points per angstrom. Changing the grid size did not affect the result. A probe radius of 1.4 Å was chosen. Periodic boundary conditions

were applied with the option "coulombic" and the convergence criterion was set to 0.001 kT/e. Both linear and non-linear iterations were set to 1000. The dielectric constant of the truncated model (ε_{in}) was taken as 4.0, [31] and that of the solvent water (ε_{out}) was taken as 80.0. [32]. Performing the above iterations, the electrostatic contribution towards the free energy change of the reduction reaction (ΔG_{el}), can be obtained. The non-electrostatic contribution ($\Delta G_{non\text{-}el}$) can be obtained by employing the DPCM method at ROB3LYP/6-31G(d) level on the 4 Å extracted structure. The same value of $G_{non\text{-}el}$ was obtained for both the neutral and charged species.

The redox reactions considered are as follows :

$$PC^{+}(aq) + e^{-}(aq) \rightarrow PC(aq) \quad (26)$$

$$Chl(sol) \rightarrow Chl^{+}(sol) + e^{-}(g) \quad (27)$$

$$Chl(sol) + e^{-}(g) \rightarrow Chl^{-}(sol) \quad (28)$$

$$Pheo(DMF) + e^{-}(g) \rightarrow Pheo^{-}(DMF) \quad (29)$$

$$Pheo(DMF) + 2e^{-}(g) \rightarrow Pheo^{2-}(DMF) \quad (30)$$

$$Pheo(Thylakoid) + e^{-}(g) \rightarrow Pheo^{-}(Thylakoid) \quad (31)$$

The redox potential values calculated for the above reactions using the methods as described above are shown in Table 1.

Table 1. Calculated and observed mid-point potential by explicit solvent treatment

Reaction	Mid-point redox potential (V)	
	Calculated	Observed
(26)	0.376 ± 0.038	0 379
(27)	0.75 ± 0 32	0.76
(28)	−1.18 ± 0 31	−1 04
(29)	−0 92 ± 0 27	−0.9
(30)	−1.34 ± 0.25	−1.25

We have successfully obtained the reduction potential values of Plastocyanin in water [7(g)], Chlorophyll-*a* in acetonitrile [7(h)] and Pheophytin-*a* by adopting the QM/MM method. The QM/MM calculations gave the redox potential of plastoquinone as 0.376 ± 0.038 V which is in good agreement with the experimental value of 0.379 V. The QM/MM/MD + Born/Onsager/Debye-Hückel method gave the standard oxidation and reduction potential of Chl-*a* as 0.75 ± 0.32 V and −1.18 ± 0.31 V respectively. These are also in agreement with the experimental value of 0.76 and −1.04 V respectively. Further, the QM/MM/MC + Born/Onsager/Debye-Hückel method gave the one- and two- electron reduction potential values of Pheophytin-*a* as −0.92 V and −1.34 V. These values are in good agreement with the experimentally reported values of

−0 9 V and −1.25 V respectively [33]. The ΔG^0_{red} calculated by DFT-DPCM method and the reduction potential calculated from eq. (25) are given in Table 2 where the error in the calculation of ΔG^0_{red} is the inherent uncertainty associated with the application of QM on large molecules and its magnitude is about 4 kcal/mol.

Table 2. Calculation of the absolute free energy of reduction (ΔG^0_{red}) and E^0_{red} of Pheophytin-*a* in DMF by DFT-DPCM nethod. We have used 1a.u = 27.2116 eV [8]

Reaction	ΔE_{DPCM}	$\Delta E_{thermal}$	$-T\Delta S_{mol}$	ΔG^0_{red}[a]	Midpoint	$E^0_{red}(V)$
		(eV)			calcd	obsd
Pheo(DMF) + e^-(g) → $Pheo^-$(DMF)	−3 222	−0 079	−0 027	−3 328	−1 032	−0 9
	±0.173[a]			±0 173	±0 173	
Pheo(DMF) + $2e^-$(g) → $Pheo^{2-}$(DMF)	−5 935	−0 158	−0 019	−6 112	−1 304	−1 25
	±0 173			±0 173	±0 173	

[a] $\Delta G^0_{red} = \Delta E_{DPCM} + \Delta E_{thermal} - T\Delta S_{mol}$

The DFT-DPCM method gave the E^0 values as −1.03 V and −1.30 V respectively.

Within the thylakoid membrane, the total free energy change of the one-electron reduction process (ΔG^0_{red}) is shown in Table 3. The corresponding calculation of the reduction potential (E^0_{red}) is given in Table 4.

Table 3. Electrostatic contribution to the free energy of the system (*i e* Pheophytin and its neighbors which are at a radial distance of 4 Å from it) computed using FDPB solver employing the Delphi software [27]

Free energy of electrostatic interaction (G_{el}) in eV		ΔG_{el} (eV)
Pheo-*a*	Pheo-*a*	
−12 080	−15.861	3 781

Table 4. Calculation of the absolute free energy of reduction (ΔG^0_{red}) and E^0_{red} of Pheophytin-*a* within the membrane $\Delta G_{non\text{-}el}$ was computed employing DPCM solvation method at ROB3LYP/6-31G(d) level on the pdb geometry We have taken ε_{in} = 4 0 and ε_{out} = 80.0

ΔG_{el}	$\Delta G_{non\text{-}el}$	ΔG^0_{red}[a]	Midpoint $E^0_{red}(V)$	
	(eV)		calcd.	obsd
−3.781	0 0	−3 781	−0.58	−0 61

[a] $\Delta G^0_{red} = \Delta G_{el} + \Delta G_{non\text{-}el}$

The FDPB method along with the DFT-DPCM technique gave the reduction potential value of Pheo-*a* within the thylakoid membrane as −0.58 V. This is in close agreement with the experimentally reported value of −0.61 V [34].

In conclusion, theoretical evaluation of the redox properties of solvated species is a tedious process that requires an extremely detailed approach, especially since the molecule-medium interaction energy plays a major role in determining the redox behavior. The reduction potentials are generally small quantities, of the order of 10^{-2} a.u., and a slight lack of accuracy in the calculation can result in a large error in the

calculated number. The explicit solvation model in general leads to a closer agreement with the observed values. This is understandable, because here the solvent molecules are explicitly considered and further, their dynamical nature accounts for fluctuations (the δV effect). Nevertheless, the DPCM method is computationally much faster. For instance, for neutral Pheo-86, the ONIOM calculation took 96 CPU hours in an Intel Xeon 3.2 GHz server with 4 GB of virtual memory space, the MC computation needed nearly 50 CPU hours, while the DFT-DPCM calculation required about 89 CPU hours. In a rigid condensed phase like a biological membrane where the medium molecules do not have the translational and rotational freedom, the δV effect is quite small. Use of an average dielectric constant for the DPCM method can give rise to a close agreement with the observed value. However, a small change in the assumed value of the dielectric constant may cause a large change in the calculated potential.

Acknowledgment

NM gratefully acknowledges financial support from Council of Scientific and Industrial Research.

References

[1] B Svensson, C Etchebest, P Tuffery, P Van Kan, J Smith and S Styring *Biochemistry* **36** 14486 (1996), M H M Olsson and U Ryde *J. Biol. Inorg. Chem.* **4** 654 (1999); P J O'Malley and S J Collins *J. Am. Chem Soc.* **123** 11042 (2001); U Ryde, M H M Olsson and Kristine Pierloot *Theoretical and Computational Chemistry* **9** 1 (2001); E Sigfridsson, M H M Olsson and U Ryde *J. Phys. Chem.* **B105** 5546 (2001), R A Torres, T Lovell, L Noodleman and D A Case *J. Am. Chem. Soc.* **125** 1923 (2003); M H M Olsson, G Hong and A Warshel *J. Am. Chem. Soc.* **125** 5025 (2003)

[2] R A Torres, T Lovell, L Noodleman and D A Case *J. Am. Chem. Soc.* **125** 1923 (2003); L Noodleman, *J. Chem. Phys.* **7** 5737 (1981)

[3] M H M Olsson, G Hong and A Warshel *J. Am. Chem. Soc.* **125** 5025 (2003)

[4] S Corni, F D Rienzo, D E Felice and E Molinari *Theoretical Biochemistry and Biophysics* **102** 328 (2004), L Y Zhang and R A Friesner *J. Phys. Chem.* **99** 16479 (1995); J Fajer, M S Davis, D C Brune, L Spaulding, D Borg and A Forman *Brookhaven Symp. Biol.* **28** 74 (1976); M S Davis, A Forman, L K Hanson and J Fajer *J. Phys. Chem.* **83** 3325 (1979); J Heimdal, K P Jensen, A Devarajan and U Ryde *J. Biol. Inorg. Chem.* **12** 49 (2007)

[5] M D Newton *J. Chem. Phys.* **58** 5833 (1973); M D Newton *Annual Rev. of Phy. Chem.* **35** 437 (1984); A Kornyshev, M Newton, J Ulstrup and B Sanderson *Chem. Phys.* **319** 1 (2005)

[6] W W Parson and A Warshel *Chem. Phys.* **296** 201 (2004); *J. Phys. Chem.* **B108** 10474 (2004)

[7] S N Datta and S Priyadarshy *Chem. Phys. Lett.* **173** 360 (1990); B Mallik and S N Datta *Int. J. Quantum Chem.* **52** 629 (1994); S N Datta and R Deshpande *Ind. J. Pure Appl. Phys.* **35** 483 (1997); S N Datta and B Mallik *J. Phys. Chem.* **B101** 4171 (1997); S N Datta, V Nehra and A Jha *J. Chem.* **B103** 8768 (1999); S N Datta, B G S Prabhakar and V Nehra *J. Phys. Chem.* **B103** 2291 (1999); S N Datta, P V Parendekar and R C Lochan *J. Phys. Chem.* **B105** 1442 (2001); S N Datta, J Sudhamsu and A Pandey *J. Phys. Chem.* **B108** 8007 (2004); A Pandey and S N Datta *J. Phys. Chem.* **B109** 9066 (2005)

[8] S N Datta and B Mallik *Int. J. Quantum Chem.* **61** 865 (1997); S N Datta and B Mallik *Int. J. Quantum Chem.* **53** 37 (1995).

[9] S N Datta and N Mehta *J. Phys. Chem.* **B111** 7210 (2007)

[10] M Born *Z. Phys.* **1** 45 (1920)

[11] L Onsager *J. Am. Chem. Soc.* **58** 1486 (1936)

[12] J Simons *Int J Quantum Chem* **13** 553 (1978)

[13] R Kubo and K Tomita *J Phys Soc* Japan **9** 888 (1954), R Kubo *J Phys Soc* Japan **12** 570 (1957), R Zwanzig *Phys Rev* **124** 983 (1961), H Mori *Prog Theoret Phys* **33** 423 (1965)

[14] A Banerjee and J Simons *J Chem Phys* **68** 415 (1978), J McHale, A Banerjee and J Simons *J Chem Phys* **69** 1406 (1978), A Banerjee and J Simons *J Chem Phys* **69** 5538 (1978), A Banerjee and J Simons *J Chem Phys* **71** 60 (1979), J McHale and J Simons *J Chem Phys* **72** 425 (1980), A Banerjee and J Simons *J Amr Chem Soc* **103** 2180 (1981)

[15] J McHale and J Simons *J Chem Phys* **70** 4974 (1979)

[16] S N Datta *J Phys Chem* **A109** 11417 (2005)

[17] S N Datta and A Panda *Int J Quantum Chem* **105** 84 (2005)

[18] S N Datta, N Mehta A Panda and S Sengupta *J Phys Chem* **B110** 14524 (2006) S N Datta, N Mehta, A Panda and A S Roy *J Phys Chem* **B111** 919 (2007)

[19] M Svensson, S Humbel, R D J Froese, T Matsubara, S Sieber and K Morokuma *J Phys Chem* **100** 19357 (1996)

[20] H Reiss and A Heller *J Phys Chem* **89** 4207 (1985), A Lewis, J A Bumpus, D G Truhlar and C J Cramer *J Chem Ed* **81** 596 (2004)

[21] Gaussian 03, Revision C 02, M J Frisch, G W Trucks H B Schlegel, G E Scuseria, M A Robb, J R Cheeseman, J A Montgomery (Jr), T Vreven, K N Kudin, J C Burant, J M Millam, S S Iyengar, J Tomasi, V Barone, B Mennucci, M Cossi, G Scalmani, N Rega, G A Petersson, H Nakatsuji, M Hada, M Ehara, K Toyota, R Fukuda, J Hasegawa, M Ishida, T Nakajima, Y Honda, O Kitao, H Nakai, M Klene, X Li, J E Knox, H P Hratchian, J B Cross, V Bakken, C Adamo, J Jaramillo, R Gomperts, R E Stratmann, O Yazyev, A J Austin, R Cammi, C Pomelli, J W Ochterski, P Y Ayala, K Morokuma, G A Voth, P Salvador, J J Dannenberg, V G Zakrzewski, S Dapprich, A D Daniels, M C Strain, O Farkas, D K Malick, A D Rabuck, K Raghavachari, J B Foresman, J V Ortiz, Q Cui, A G Baboul, S Clifford, J Cioslowski, B B Stefanov, G Liu, A Liashenko, P Piskorz, I Komaromi, R L Martin, D J Fox, T Keith, M A Al-Laham, C Y Peng, A Nanayakkara, M Challacombe, P M W Gill, B Johnson, W Chen, M W Wong, C Gonzalez and J A Pople Gaussian, Inc , Wallingford CT, (2004)

[22] T Vreven, K S Byun, I Komáromi, S Dapprich, J A Montgomery, K Morokuma and M J Frisch *J Chem Theory and Comput* **2** 815 (2006)

[23] A K Rappé, C J Casewit, K S Colwell, W A Goddard, (III) and W M Skiff *J Am Chem Soc* **114** 10024 (1992), A K Rappe and W A Goddard, (III) *J Phys Chem* **95** 3358 (1991)

[24] Hyper Chem Professional Release 7 01 for Windows, Hypercube Inc , Gainesville, FL, (2002)

[25] J O M Bockris and A K N Reddy in *Modern Electrochemistry* (New York and London Plenum Press) (1998)

[26] J Tomasi, B Mennucci and R Cammi *Chem Rev* **105** 2999 (2005)

[27] W Rocchia, E Alexov and B Honig *J Phys Chem* **B105** 6507 (2001)

[28] W Rocchia, S Sridharan, A Nicholls, E Alexov, A Chiabrera, B Honig *J Comp Chem* **23** 128 (2002)

[29] G Vriend *J Mol Graph* **8** 52 (1990)

[30] Delphi V 4, release 1 0, Accelrys Inc , Pisa, Italy, (2001)

[31] H Ishikita and E Knapp *FEBS Letters* **579** 3190 (2005)

[32] H Ishikita and E Knapp *JACS* **127** 1963 (2005)

[33] A A Kazakova, B A Kisselev and Y N Kozlov *Bioelectrochemistry and Bioenergetics* **21** 367 (1989)

[34] H Scheer *Chlorophylls* (London CRC) (1990)